THE ASTROPHYSICAL JOURNAL, 545:512–523, 2000 December 10


# ANOTHER VIEW OF THE EIT WAVE PHENOMENON

C. DELANNÉE
NASA/Goddard Space Flight Center, Mail Code 682.3, Greenbelt, MD 20771
*Received 2000 January 18; accepted 2000 July 5*

## ABSTRACT

This paper investigates three different EIT waves. The events occurred on 1997 November 3 at 10:31 UT, on 1998 January 27 at 22:19 UT, and on 1998 June 13 at 15:23 UT and were observed with EIT on board the *Solar and Heliospheric Observatory* (*SOHO*) using the 195 Å filter that contains an Fe XII line.

The three events show the following similar structures:

1. A flare in an active region.
2. A bright front that can lie at the same location for several hours.
3. A first dimming located between the bright front and the flare.
4. A second dimming located between the bright front and a magnetic dipole located in the opposite hemisphere.
5. A third dimming located in an active region located in the opposite hemisphere.
6. Brightenings or dimmings of transequatorial loops that connect the flaring active region to an active region located in the opposite hemisphere.

We propose that the appearance of the above features is strongly related to magnetic field topology. Most of the EIT waves are associated with a coronal mass ejection (CME). Moreover, the presence of a flare is not a necessary condition to produce an EIT wave since only eruptive flares that are associated with CMEs are associated with a wave. Therefore, we suggest that the EIT-wave phenomenon is more closely related to the magnetic field evolution involved in CMEs than to wave propagation driven by solar flares.

*Subject headings:* Sun: corona — Sun: flares — Sun: magnetic fields

## 1. INTRODUCTION

Coronal mass ejections (CMEs) are known to be associated with several signatures observed on the disk: transient coronal holes, EIT waves, flares, and prominence eruptions or filament *disparitions brusques*. Transient coronal holes are dimming areas appearing suddenly (at the timescale resolution of the instruments) when a CME occurs and fades on timescales between a few tens of minutes to a day. They are interpreted as a density decrease (Hudson, Acton, & Freeland 1996; Thompson et al. 1998). Some dimming areas are described as double structures extending diagonally in opposite directions from the postflare loop arcade (Manoharan et al. 1996; Thompson et al. 1998; Zarro et al. 1999). These dimmings find their origin near the ends of ejected filaments. On the other hand, faint dimmings also can be located along the filament channel (Solodyna, Krieger, & Nolte 1977; Khan et al. 1998). Some transequatorial loops also can be observed ejecting (Maia et al. 1999; Wills-Davey & Thompson 1999; Khan & Hudson 2000). Large dimming areas have been observed at their ejection sites (Khan & Hudson 2000). Manoharan et al. (1996) found transient coronal holes located at footpoints of large-scale transequatorial loops that overlaid a twisted flux rope that had erupted.

Flares are intensity increasing on a short timescale in multiple wavelengths. Homologous flares (Martres 1989) have very similar morphologies, intensities, and durations. Most flares are associated with complex magnetic topologies such as a bald patch (location where the magnetic field lines are tangent to the photosphere; Bungey, Titov, & Priest 1996; Aulanier et al. 1998; Delannée & Aulanier 1999), null points (Karpen et al. 1998; Antiochos, DeVore, & Klimchuk 1999), or quasi-separatrix layers (Démoulin et al. 1997; Milano et al. 1999; Titov & Démoulin 1999). Flares are driven by processes of reconnection of magnetic field lines that release the energy of the magnetic configuration. Some of these flares imply the reconfiguration of the magnetic topology in which some magnetic field lines open (Amari et al. 1996; Antiochos et al. 1999).

EIT waves are observed as moving bright fronts in coronal lines. The velocities of the bright fronts are in the range of 300–400 km $s^{-1}$. They are presumed to be the coronal counterpart of Moreton waves observed in Hα—at least one case shows both chromospheric and coronal emissions (Thompson et al. 2000). If a flare related to an EIT wave occurred close to the limb, then, in some cases, the bright front of the wave can be observed partly above the limb (Thompson et al. 1999; Delannée, Delaboudinière, & Lamy 2000). The morphology of the wave is usually described as a semicircular thread (Thompson et al. 1998; Wills-Davey & Thompson 1999; Delannée et al. 2000). Wills-Davey & Thompson (1999) have shown in one case that the wave is contained within large-scale magnetic field lines connecting two active regions located each in opposite solar hemispheres. In that case, some spicules do not appear to move when the wave front passes through them; therefore the minimum height of the wave is supposed to be at 15 Mm (average height of spicules). Both EIT and Moreton waves have been interpreted as coronal waves driven by the energy release associated with the production of a flare (Uchida 1968).

We propose in this paper a different interpretation of the EIT waves. The method of study is not new, but we point out some facts that are usually put aside. We recall the

results already published in Delannée & Aulanier (1999) and generalize these previous observational results by analyzing two new examples of EIT waves. In § 2 the methods of analysis are described. These three cases are presented in § 3. A summary of the observed structures and a discussion on the phenomenology is given in § 4. We conclude on the new view of the EIT waves in § 5.

## 2. THE TOOLS FOR THE STUDY

The EIT instrument (Extreme-Ultraviolet Imaging Telescope, Delaboudinière et al. 1995) on board the *Solar and Heliospheric Observatory* (*SOHO*) observes the solar surface in different coronal wavelengths. The bandpass centered on 195 Å used in this analysis comprises a Fe XII line emitted at $1.2 \times 10^6$ K at typical coronal densities. Images of the whole Sun were obtained approximately every 17 minutes with a 5.″24 spatial resolution. The study of these events is oriented to find out if some stationary structures appear on the way to propagation of the waves, so the images are corrected to remove the effects of the differential rotation. All structures appearing during the events are very faint. To highlight them, difference images were computed by subtracting a base image obtained just before each event (at 10:22 UT on 1997 November 3, at 21:41 UT on 1998 January 27, and at 15:02 UT on 1998 June 13). We took special care to distinguish the features that can be related to the propagation of the wave from the ones that are due to other coronal activities such as small changes in brightness of bright points or of loops linking two polarities of the same active region or the appearance of brightenings related to other CMEs by comparing the images with the difference images and by tracking the evolution of the structures. A subfield of view (1641″ × 1522″ on 1997 November 3, 1345″ × 1408″ on 1998 January 27, and 969″ × 1802″ on 1998 June 13) comprising all the structures involved in the events is analyzed.

The *Transition Region and Coronal Explorer* (*TRACE*; Handy et al. 1999) observed the 1999 June 13 event using three filters centered on 195 Å (Fe XII), 173 Å (Fe IX), and 1216 Å (H I Lyα) at a time resolution of approximately 2 minutes. The field of view (512″ × 512″) was centered at N10°, W21°. The spatial resolution is 0.″998 in 195 Å and 1216 Å and 0.″499 in 173 Å.

The Large Angle and Spectrometric Coronagraph (LASCO) C2 (Bruekner et al. 1995) on board *SOHO* observed the CMEs associated with each event with a spatial resolution of 11.″14 pixel$^{-1}$ and a time resolution of about 1 hr. The field of view ranges from 2 to 6 $R_\odot$.

All the events are related to structures observed in Hα using the Meudon spectroheliograph synoptic observations. The Michelson and Doppler Instrument (MDI) provided the magnetograms that are helpful to describe the different magnetic structures involved in the studied events. The *Geosynchronous Operational Environmental Satellite* (*GOES*) provided the intensity and the time of the maximum of the flares. However, no detailed analysis of the Hα and magnetogram observations and of the X-ray intensity variations due to the flares is done in this paper.

## 3. THE EVENTS

We present the analysis of three observations of events that occurred on different dates (1997 November 3, 1998 January 27, and 1998 June 13) from different active regions (AR 8100, AR 8144, and AR 8237) but that present some strong similarities. The evolution of the structures that appeared are described in this section. Stationary features of EIT waves are highlighted. These kinds of structures were found in a previous study that we will recall in § 3.1. The two other events are presented in §§ 3.2 and 3.3 to demonstrate that these stationary structures are not uniquely observed in the first case. Since we will show how the flares, the EIT waves, and the CMEs are all related and present different parts of the same phenomenon, the term "event" will refer to the appearance of the structures. All the dates and times given refer to the first EIT image on which an event appeared.

### 3.1. *1997 November 3*

This event was studied in detail by Delannée & Aulanier (1999). It is one of the eight events that appeared on three consecutive days (1997 November 3–6; Delannée et al. 2000). All of these events are found to be related to a CME observed by LASCO C2. Of these events, six are found to be homologous, which means that they show similar evolution of similar structures located in roughly the same regions. For all of the eight events, a flare appeared in AR 8100 (S19°, W12°). For the six homologous cases, the flare is clearly located near a parasitic polarity.

In the following discussion the conclusion of the detailed analysis of the event that appeared on 1997 November 3 at 10:43 UT and was published in Delannée & Aulanier (1999) is recalled, reminding us that six other events showed similar behavior. The same first image of the flare shows a bright front of an EIT wave. One dimming area appeared between the bright front and the active region. The second image of the event shows that a part of the bright front remained at the same position. This bright front was not due to another flare, since none are detected either in EIT or in *GOES* data between the two images, but was rather due to the stationarity of the structure. Two dimming areas had developed between the bright front and AR 8102 (N30°, E12°). Three transequatorial loops linking AR 8100 and AR 8102 show brightenings. The third image indicates that the bright front, the dimming areas located near AR 8100, and the bright transequatorial loops had disappeared. The dimming areas located near AR 8102 were less pronounced. Only three of the 50 flares produced in AR 8100 on 1997 November 3 throughout the day were associated with an EIT wave, indicating that flares are not the primary cause for production of a bright front but that other conditions are needed to produce in the same event a flare and an EIT wave.

Delannée & Aulanier (1999) computed potential extrapolation of magnetic field lines and compared the results with the observed features. The flare occurred near the separatrix of the magnetic field. They proposed that the bright front may be produced by the sudden expansion of a part of the magnetic field lines forming the separatrix when the flare occurred. This expansion would lead to a compression of the plasma and its brightening. On each side of the bright front, dimmings were developed because of the decrease in density at the locations where the magnetic field lines expanded (cf. Fig. 8 in Delannée & Aulanier 1999).

### 3.2. *January 27*

On 1998 January 27 at 22:19 UT a similar event to the one studied in § 3.1 took place. A B2.0 class flare appeared on the first image of the event (Figs. 1 and 2*a*) in AR 8144

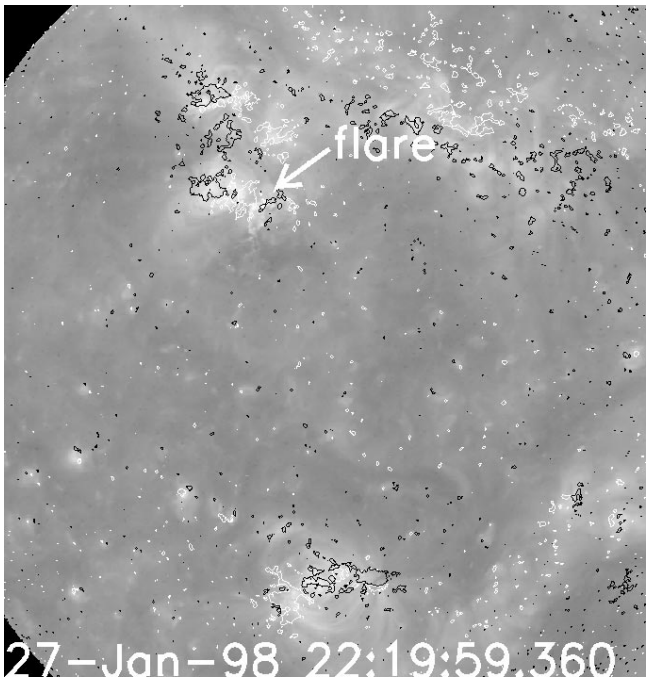


FIG. 1*a*

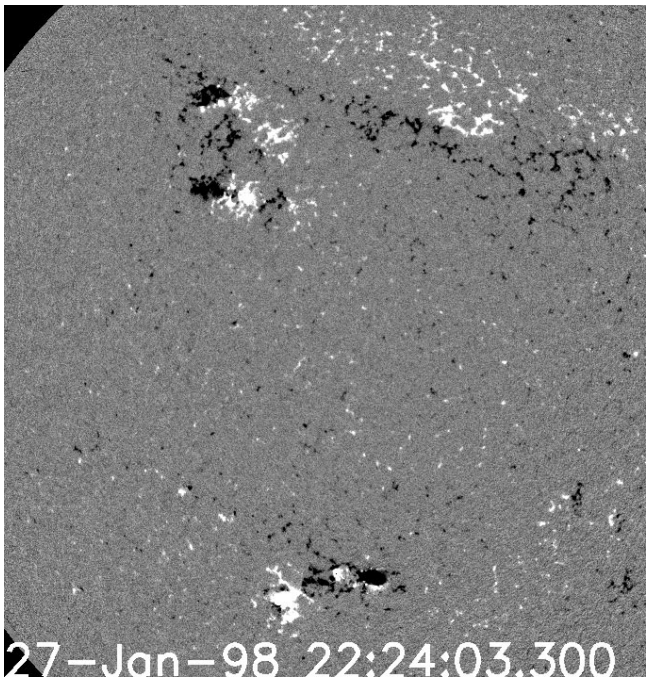


FIG. 1*b*

FIG. 1.—(*a*) Image at 22:19 UT obtained in 195 Å (Fe XII) showing EIT and overlay of MDI magnetogram (see panel *b*). A filament, located between two opposite polarities, is ejected. A flare appears. (*b*) MDI magnetogram at 22:24 UT overlaid on panel *a*.

located at N12°, E27°. *GOES* shows a peak intensity at 22:20 UT. The Hα image obtained at Meudon Observatory at 10:11 UT shows a filament at the location of the flare. By 14:59 UT the following day the filament had disappeared. Figure 1 shows small bright and dark features at the location of the filament. The dark feature may be due to the absorbing material of the ejecting filament, and the bright one may be due to the usual brightening observed at the leading edge of the ejecting filament/prominences or to some flares occurring below the filament itself. These features show that the filament may be observed while ejecting. However, no CME was detected in LASCO C2 because of insufficient data coverage.

The first EIT image of the event (at 22:19 UT, Fig. 2*a*) shows the flare, a bright front located near the equator, and a dimming area between AR 8144 and the bright front. On Figures 2*a*, 2*b*, and 2*c* the head of the arrow showing the bright front is drawn at the same location to facilitate the comparison of the location of the bright front from one image to another.

The subsequent image at 22:34 UT (Fig. 2*b*) shows that the bright front has moved slightly southward. Some parts of the bright front have disappeared, while other parts remained at the exact same location. The dimming area located between the bright front and AR 8144 has changed in shape, with additional dimmings developing in the northern and southern edges (the southern one is shown at the head of the arrow in Fig. 2*b*).

The third EIT image of the event at 23:04 UT (Fig. 2*c*) shows that the bright front faded in intensity but remained in the same shape at the same location. The southern part of the first dimming area has faded more rapidly than the dimming areas near AR 8144. Two other very faint dimming areas (intensity decrease of 5%–11%) have developed between the bright front, AR 8143 (S36°, E12°), and two filaments (near AR 8143 at S25°, E15° and at S30°, W05°). The two filaments showed intensity increase of about 10%; however, these fluctuations were possibly due to their own activity.

The last EIT image at 23:20 UT (Fig. 2*d*) shows that all dimming and brightening areas have faded, while a new dimming area has appeared in AR 8143 (Fig. 3). Some loops that were bright at 23:04 UT have faded at 23:20 UT. Their disappearance in AR 8143 where no flare is detected and located in the opposite hemisphere may imply that these loops are transequatorial loops connecting the two active regions (AR 8144 and AR 8143) that may open during the ejection leading to a coronal density decrease associated with dimming areas. However, the disappearance of these loops could also be due to some activity in the loops themselves.

### 3.3. *1998 June 13*

This event is already published in Wills-Davey & Thompson (1999), but the analysis of some other structures not done in this previous paper is presented here. The event appeared on 1998 June 13 at 15:23 UT (Fig. 4) and is associated with a *GOES* C2.9 class flare with a maximum of intensity at 15:33 UT that occurred between the eastern part of the main negative polarity and the western part of the main positive polarity regions of AR 8237 at S25°, W04° where a filament was observed in Hα. The filament was detected during its ejection as a small dark and bright evolving feature in the EIT field of view (Fig. 4) and as a dark compact feature in the three *TRACE* filters. This event was associated with a halo CME observed in white light with LASCO C2 (Fig. 5) with a leading edge moving at 190 km $s^{-1}$.

#### 3.3.1. *EIT 195 Å Observations*

The EIT 195 Å difference images show structures that are similar to those found in the previous two events. At 15:23

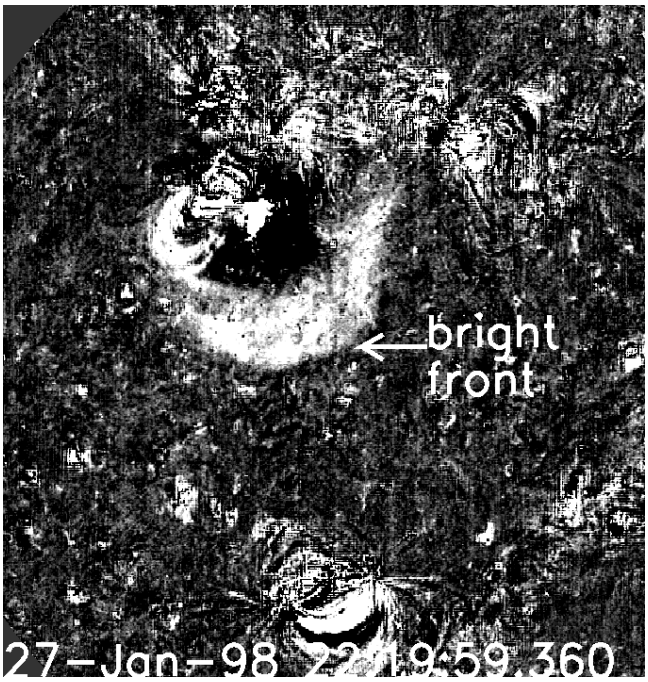


FIG. 2*a*

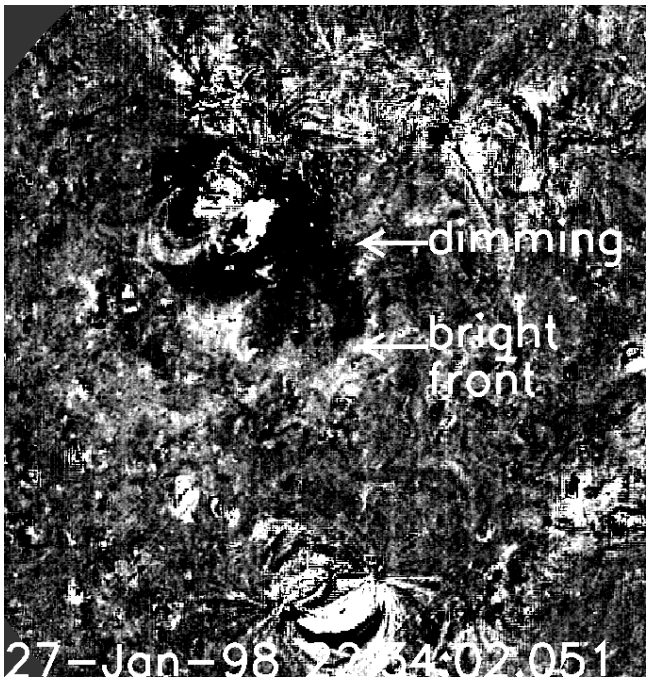


FIG. 2*b*


FIG. 2*c*


FIG. 2*d*

FIG. 2.—EIT difference images of the 1998 January 27 event in Fe XII with a base image at 21:41 UT showing the development of the structures related to the ejection: a bright front, dimmings, brightenings in two southern filaments, and a dimming area located in AR 8143 (Fig. 3).

UT (Fig. 6*a*) the flare is well visible in AR 8237 accompanied by the bright front of an EIT wave. At 15:40 UT (Fig. 6*b*) the bright front and a dimming area located between the bright front and the active region have both developed.

The bright front shows some small oscillations between 15:40 UT and 16:35 UT. Three different parts of the bright front are distinguishable (Fig. 6*b*). The western part (located at the head of the right arrow showing the bright front, Fig. 6*b*) shows a maximum displacement of 40″ toward the south. The central part of the bright front is stationary for 2 hr. The eastern part of the bright front (at the head of the left arrow showing the bright front, Figs. 6*b* and 6*c*) is bright at 15:40 UT (Fig. 6*b*), darkens at 15:53 UT (Fig. 6*c*), and brightens again from 16:02 to 16:35 UT (Figs. 6*d*–6*f*). This part is stationary for 2 hr. Three other brightenings are detected at the edge of the dimming area located near AR 8237, which appear independently of the event. The first one (b1, Fig. 6*f*) is a "bright point" whose contrast is artificially

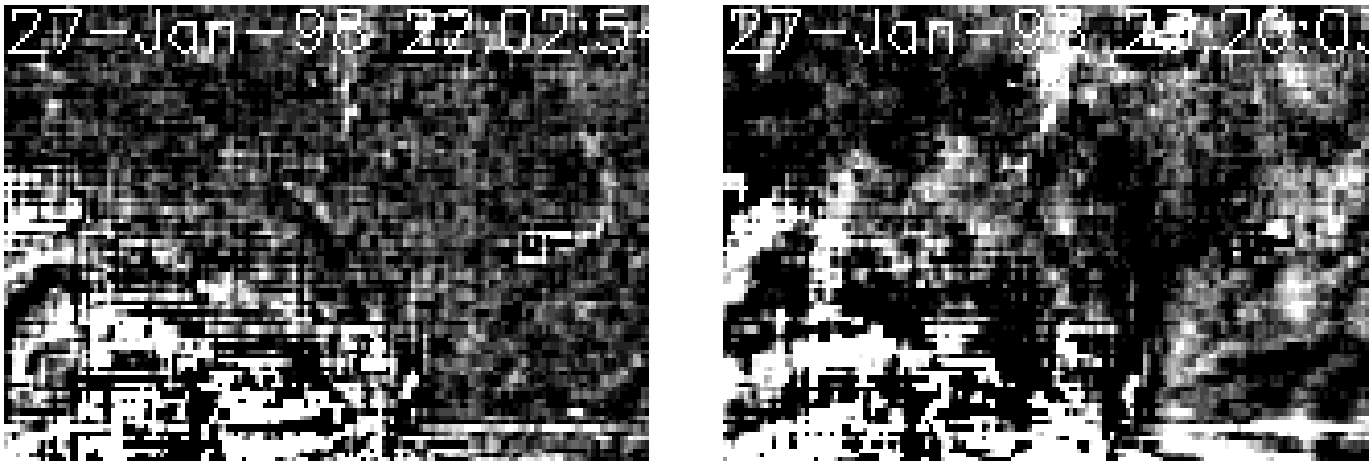


FIG. 3.—Close-up of the EIT difference images presented in the white square in Fig. 2. Several loops show a particular dimming.

enhanced because of the dimming of the surrounding areas. The two other brightenings (b2 and b3, Fig 6*f*) are both associated with the ejection of a polar crown filament (S32°, E09°) at 15:53 UT. The effects of this ejection are distinguishable from the ones of the studied ejection because of their much slower evolution.

The most prominent dimming area was located between the bright front and AR 8237 (d1, Fig 6*c*) surrounding the active region in all direction with a large extension toward the equator. The shape of this dimming area changes slightly from one image to another. Two other dimming areas are located between the bright front and two active regions in

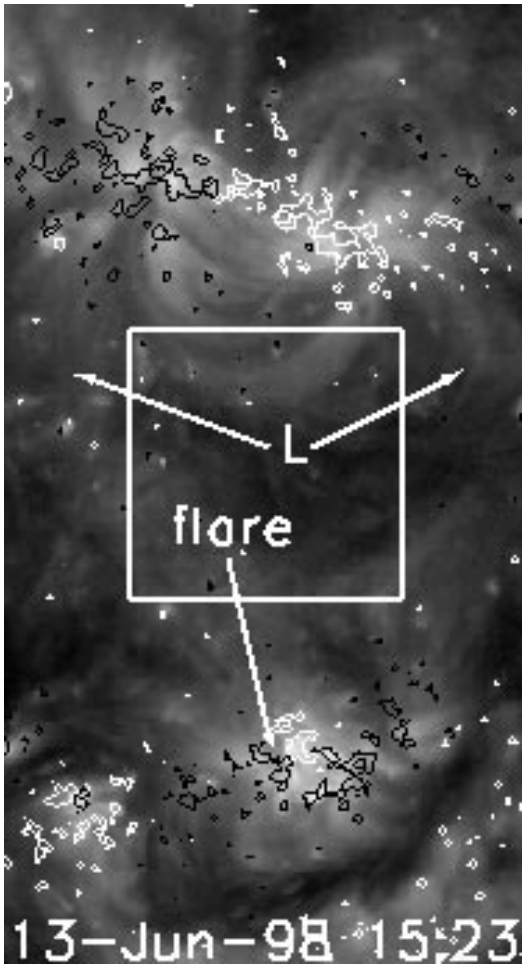


FIG. 4*a*

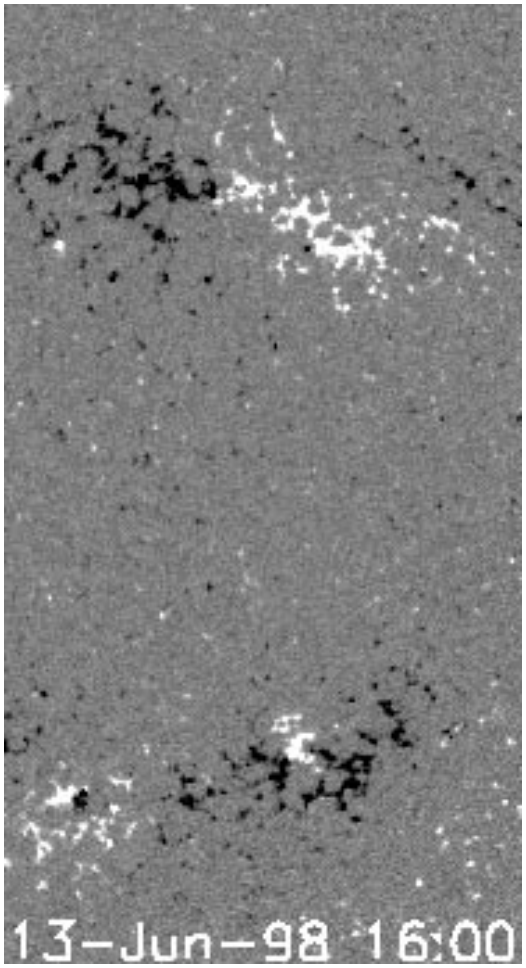


FIG. 4*b*

FIG. 4.—(*a*) Image at 15:23 UT obtained in 195 Å (Fe XII) showing EIT and overlay of the MDI magnetogram (see panel *b*). A filament, located between two opposite polarities of AR 8237, is ejected. Near this location a flare appears. (*b*) MDI magnetogram at 16:00 UT overlaid on panel *a*.

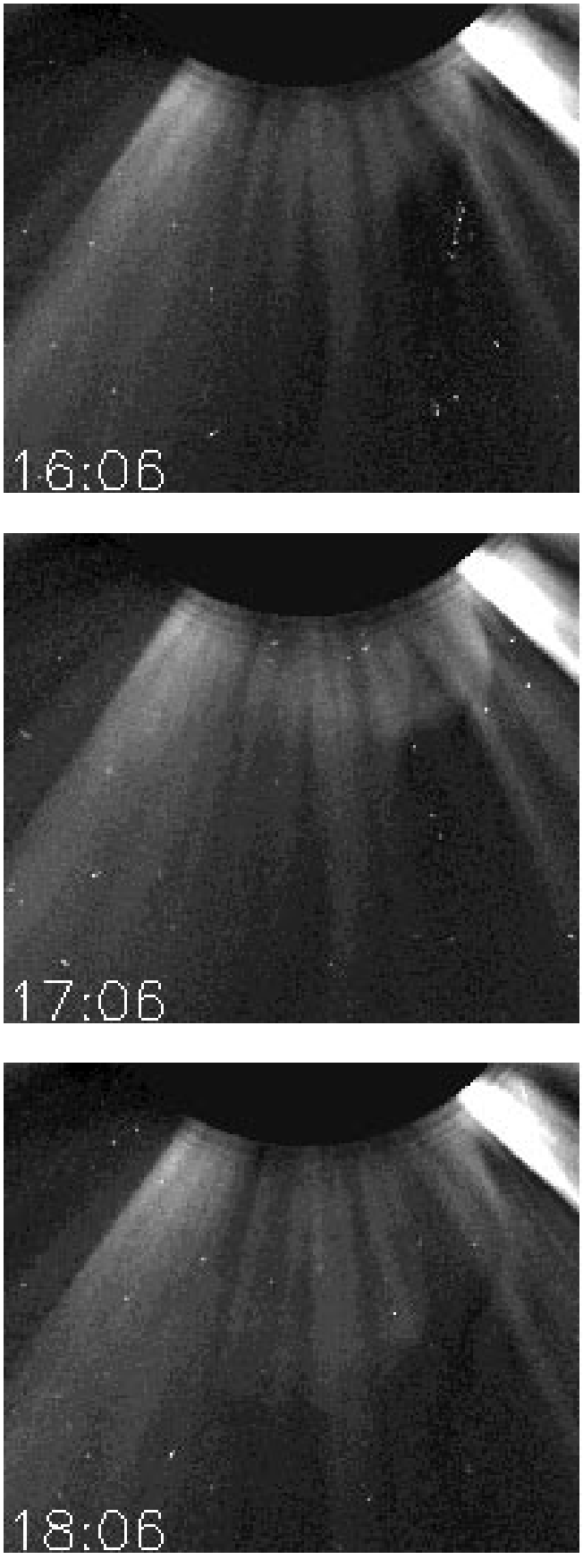


FIG. 5.—White-light observations, using LASCO C2, of the halo related to the ejection of the filament in AR 8237.

the opposite hemisphere (AR 8238 at N19°, E01° and AR 8239 at N25°, E14°). These dimmings are situated within transequatorial loops that link the northern and southern active regions. The transequatorial loops are quite well observed in the raw image (Fig. 4*a*). The footpoints of the ones linking AR 8237 to AR 8238 dimmed a lot near AR 8238 (d2, Fig. 6*c*). The mark of these dimmed loops can be followed on the images of difference.

#### 3.3.2. *TRACE 195* Å *Observations*

*TRACE* observations show similar structures with improved temporal and spatial resolution. They also reveal additional features. In 195 Å the bright front evolves as follows: Initially (between 15:27 UT—the first image showing the bright front—and 15:36 UT) the bright front is composed of an arch and a "thick" structure (Figs. 7*a* and 7*b*). Until 15:34 UT the thick structure is located at the western edge of the arch. After 15:34 UT two other parts of the thick structure develop. The arch propagates across the *TRACE* field of view at about 700 km $s^{-1}$ (Wills-Davey & Thompson 1999). It is no longer visible at 15:39 UT (Fig. 7*c*). The remaining part of the thick structure is the stationary bright front observed with EIT. The slight southward motion of the western part of the stationary bright front is confirmed. In the middle of the stationary bright front several small loops are observable with the improved *TRACE* spatial resolution. The eastern part of the stationary bright front observed in the EIT field of view here is out of the *TRACE* field of view. The loops located near the northern active regions and the ones located at the southwestern edge of the *TRACE* field of view show oscillations. The motions of the moving arch and of the oscillating loops are described in detail in Wills-Davey & Thompson (1999).

Dimmings areas are observed with *TRACE* that can be related to the ones observed with EIT. The dimming area located in the south of the bright front on *TRACE* corresponds to the northern edge of the dimming area located between the bright front and AR 8237 (the flaring active region) on EIT, and the dimming area located in the north of the bright front on *TRACE* is a part of the dimmed transequatorial loops linking AR 8237 to AR 8238 observed on EIT. The shapes of these dimming areas do not change significantly from 15:39 UT to 16:27 UT (Figs. 7*c*–7*f*).

#### 3.3.3. *TRACE Observations in the Other Wavelengths*

The *TRACE* observations in 173 Å (Fe XI) show slightly different features and different behaviors (Fig. 8). The moving arch and the stationary bright front are thinner, and the dimmings are less pronounced than in 195 Å (Fe XII). However, the oscillation of the loops is better observed. In particular, a part of a transequatorial loop (L, Figs. 8*d* and 8*e*) shows a bright feature that moves northward along the loop direction.

The *TRACE* observations obtained in 1216 Å (H I Ly$\alpha$) show several very faint small structures. The bright front is observed from 15:34 UT to 15:43 UT (Figs. 9*a* and 9*b*). The dimming lasts until 15:52 UT. The shapes of the bright front and of the dimming areas change continuously during the observations.

## 4. SUMMARY OF THE OBSERVED STRUCTURES AND DISCUSSION

We presented observations obtained using the 195 Å filter of EIT and the 195 Å, 173 Å, and 1216 Å filters of

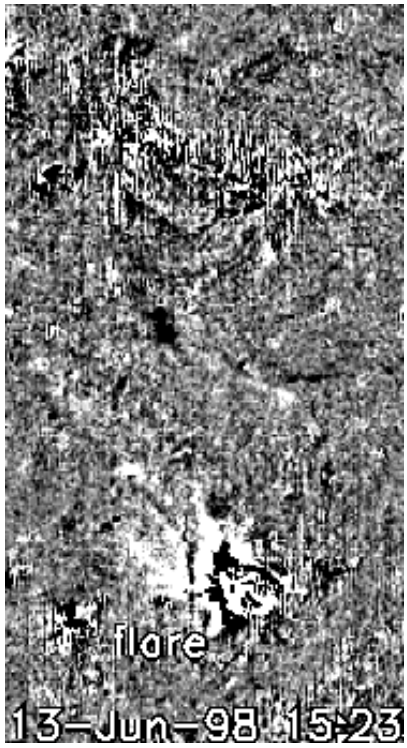


FIG. 6*a*


FIG. 6*b*

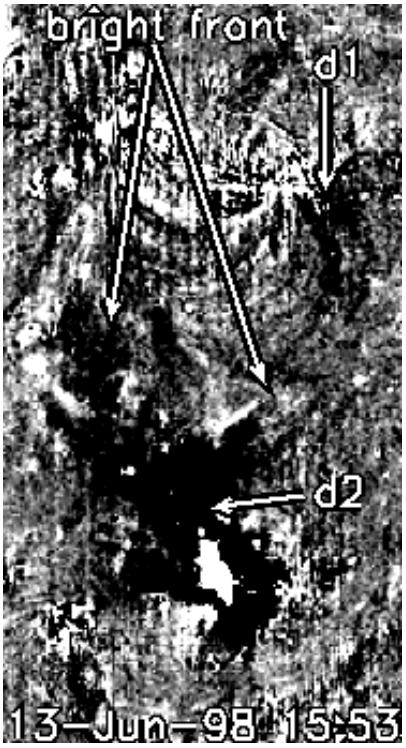


FIG. 6*c*


FIG. 6*d*


FIG. 6*e*

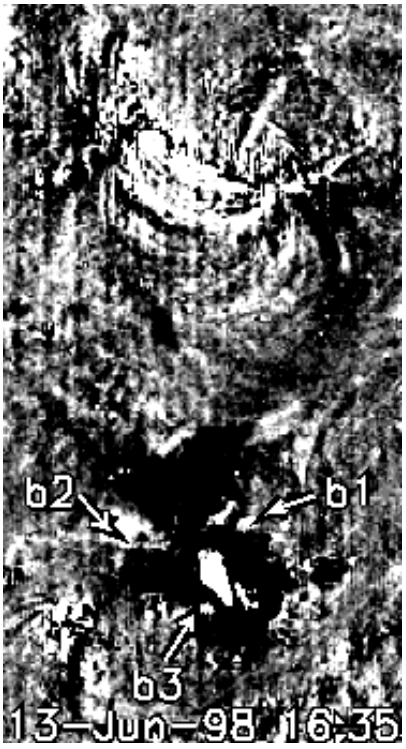


FIG. 6*f*

FIG. 6.—EIT difference images of the 1998 June 13 event in Fe XII with a base image at 15:02 UT showing the development of the structures related to the ejection: a bright front and dimmings, with dimmings evident near AR 8238.

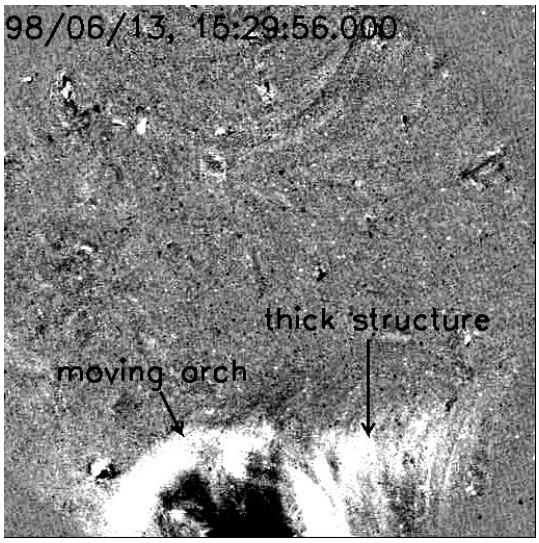


FIG. 7*a*

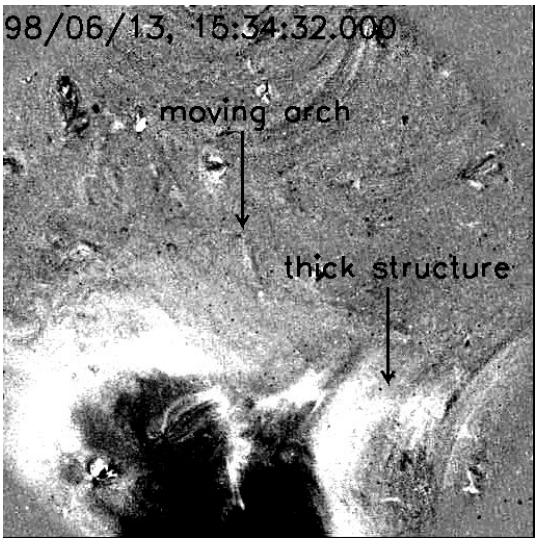


FIG. 7*b*

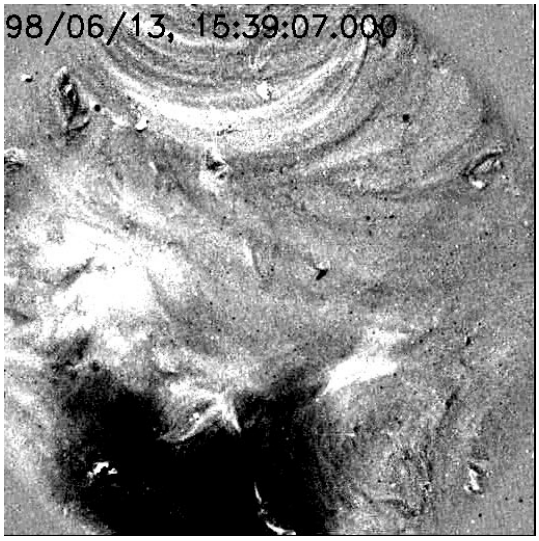


FIG. 7*c*

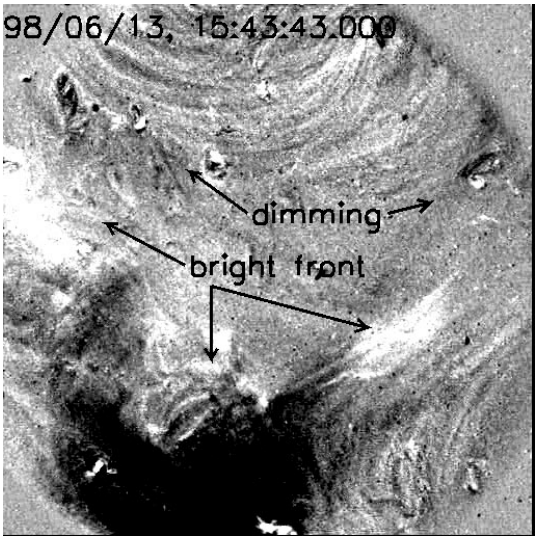


FIG. 7*d*

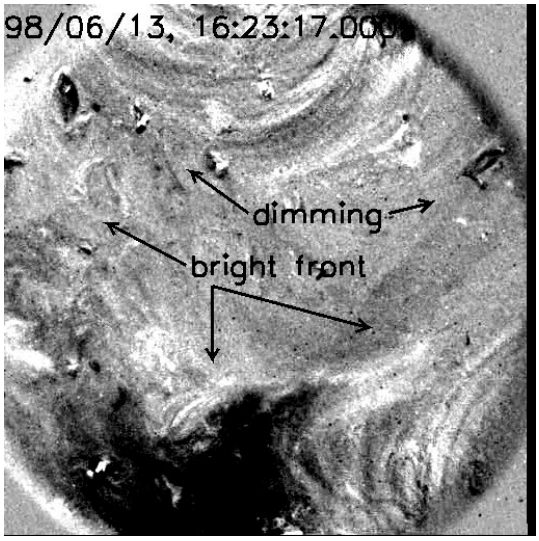


FIG. 7*e*

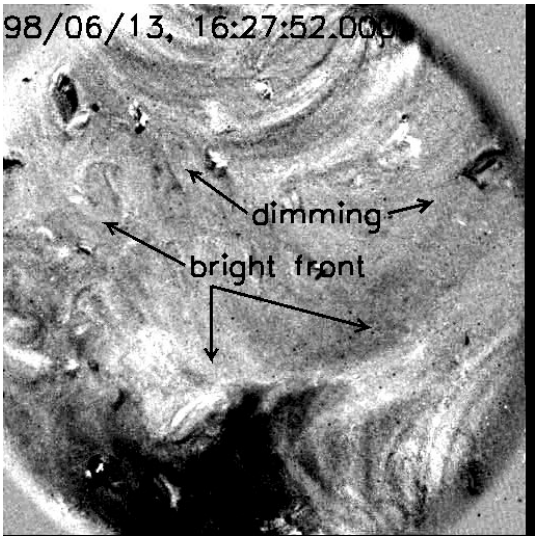


FIG. 7*f*

FIG. 7.—*TRACE* 195 Å (Fe XII) of the field of view shown in the white square on Fig. 4*a*. The bright front of the wave is observed in motion; an arch propagates through out the field of view, while a bright thick structure remains stationary.

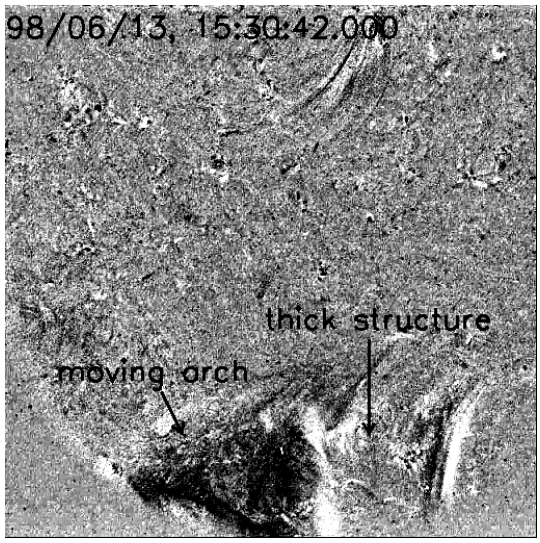


FIG. 8*a*

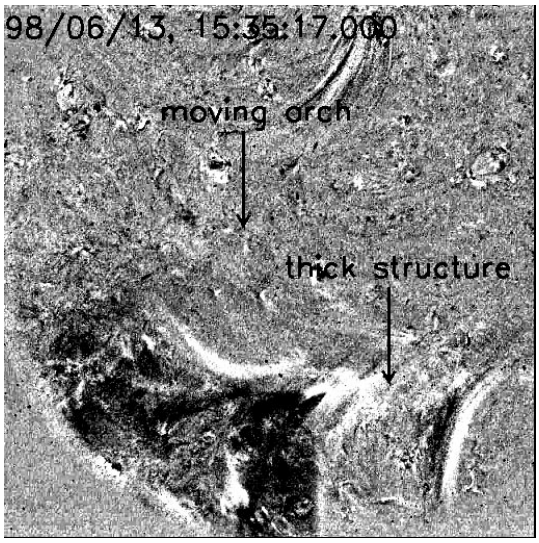


FIG. 8*b*

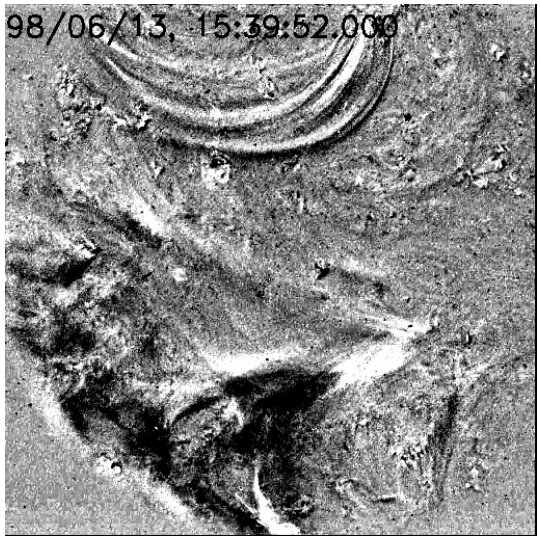


FIG. 8*c*

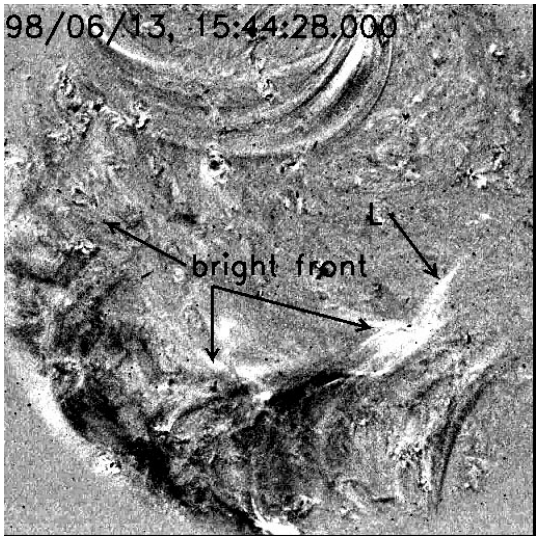


FIG. 8*d*

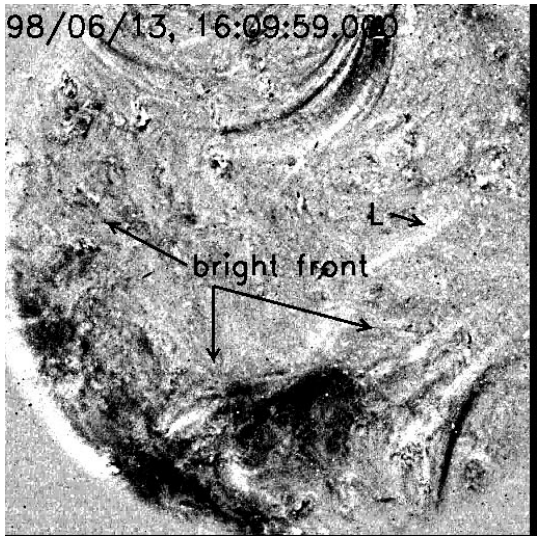


FIG. 8*e*

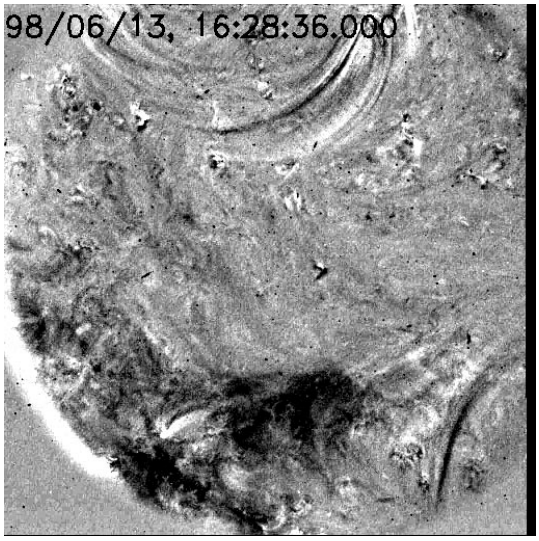


FIG. 8*f*

FIG. 8.—*TRACE* 173 Å (Fe XI). The bright front is fainter and thinner than in Fe XII. Fine loops structures are better observed oscillating, especially transequatorial loops.

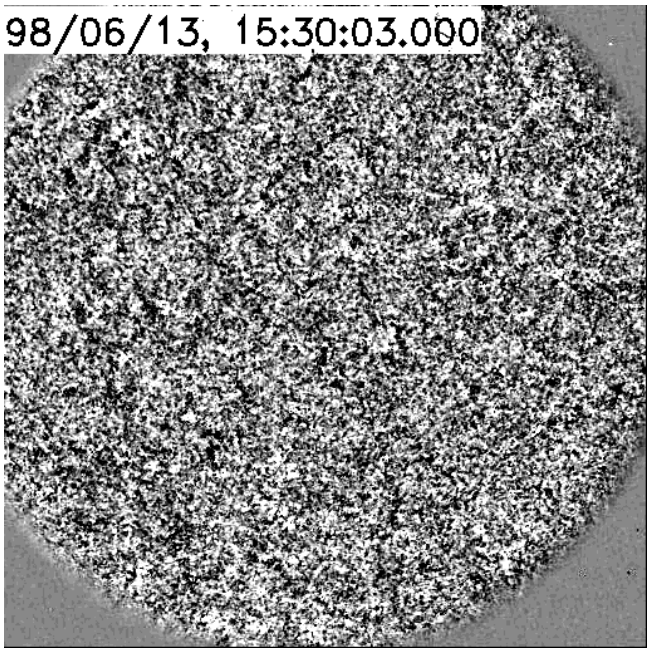


FIG. 9*a*

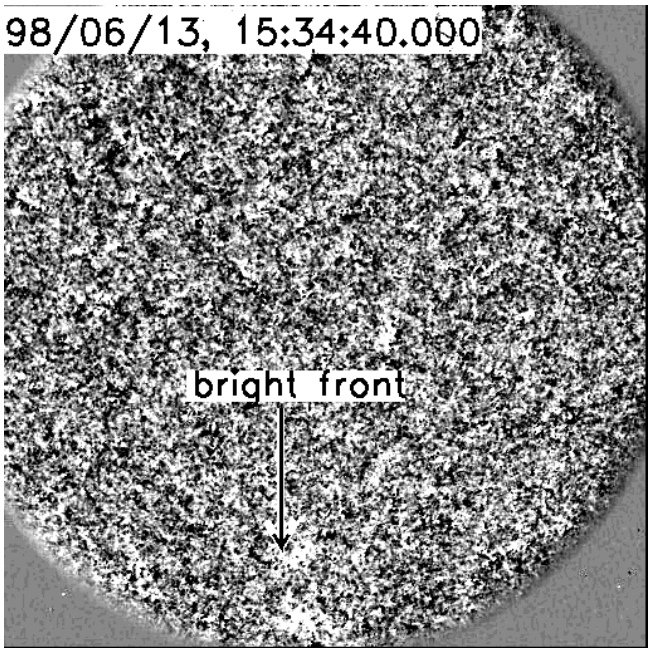


FIG. 9*b*

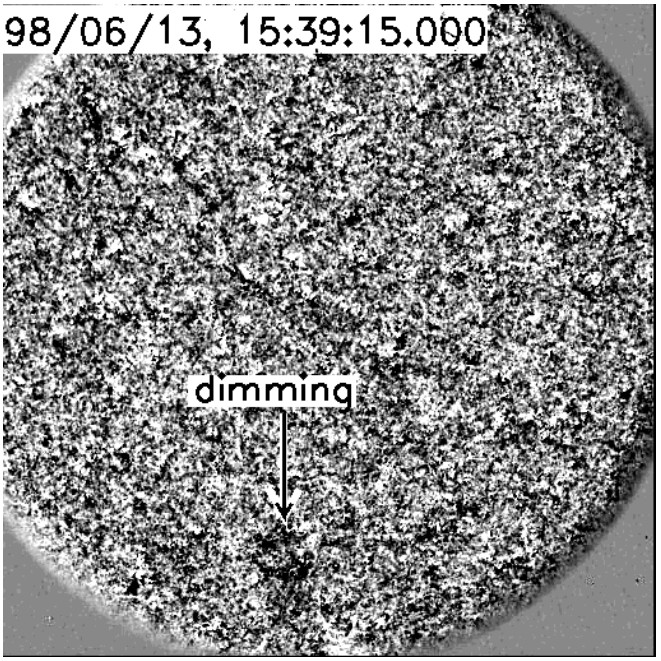


FIG. 9*c*

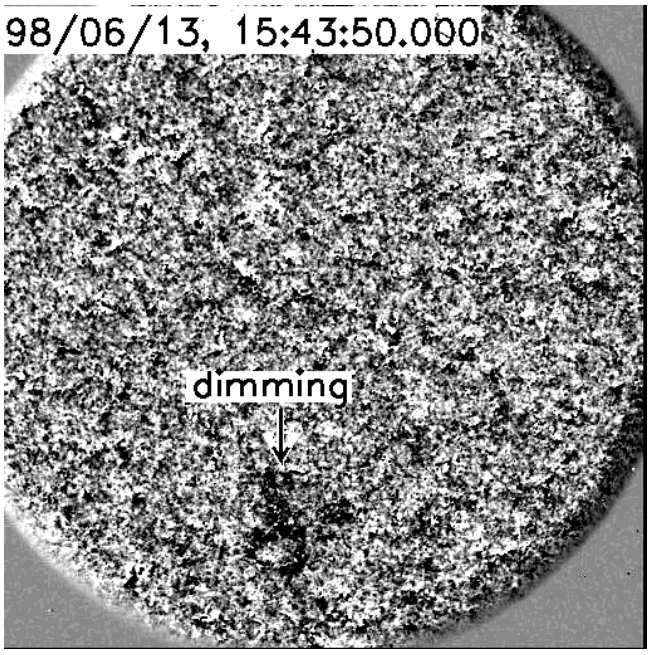


FIG. 9*d*

FIG. 9.—*TRACE* 1216 Å (H I Ly$\alpha$). Parts of the bright front and of the dimming areas are observed. Their lifetimes are approximately 10 minutes.

*TRACE* of three events that occurred in different active regions but that had the following common structures:

1. A flare is located near an active region.
2. A bright front, which appears on the same first image as the flare, starts moving. Portions of the bright front remain stationary for 17 minutes to 1 hr near the equator.
3. A first dimming area is located between the flare and the bright front.
4. A second dimming area is located between the bright front and another magnetic dipole (active region or filament) located in the opposite hemisphere.
5. A third dimming area is located near the other dipole.

In some cases, transequatorial loops connecting the flaring active region and the other magnetic dipole show motions and intensity variations.

Figure 10 summarizes the different structures appearing in a typical event.

Two events are related to an observed CME. For the third event, the LASCO C2 observations had too many data gaps at the time of the ejection in the affected region. A previous statistical study held on six consecutive days of observations by Delannée et al. (2000) concluded that 86% of bright fronts are associated with a CME. Taking into account the remark already made in Delannée & Aulanier

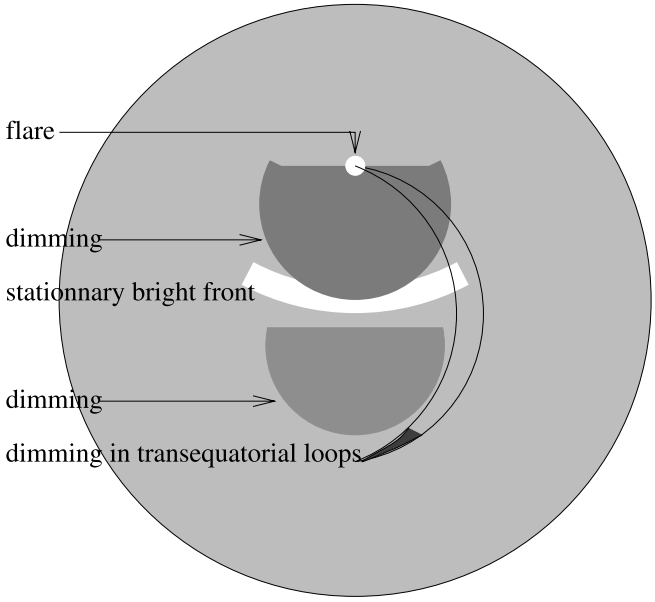


FIG. 10.—Sketch presenting all the different structures appearing in a typical event described in the paper: the flare, the dimming located between the flare and the bright front, the bright front, the dimming located between the bright front and another dipole, and the dimming in transequatorial loops linking the flare region to another dipole.

(1999) that the flares are not the only condition to produce an EIT wave/bright front, the bright front seems more likely to be related to eruptive flares that lead to a CME than to wave propagation caused by explosive energy release in flares.

The usual interpretation of the EIT wave is a fast-mode magnetoacoustic wave to explain its arch shape and the oscillation of structures on its way to propagation. However, some small spicules did not oscillate on the way of the propagation of the moving arch in the case of the 1998 June 13 event (Wills-Davey & Thompson 1999). So, the authors concluded that the moving arch is a wave propagating at 15 Mm height. In fact, the opening of magnetic field lines would produce the same effects; they would push some high loops, producing their oscillation, and pass over some low spicules. In the two hypotheses (wave or magnetic field opening) the equilibrium state of the oscillating loops will be their immobility, which would take some time to be reached. If the arch is a wave, then the location of the loops at their equilibrium state will be the same after the passage of the wave as before it. If the arch is due to the opening of magnetic field lines, then the location of the loops will be a little bit different after the expansion than before it. However, we could not use this criterion to determine which hypothesis is suited to explain the moving arch since the exact position of the new immobility of the oscillating loops could not be determined with these *TRACE* observations.

EIT observations on 1997 May 12 by Thompson et al. (1998) showed an almost circular bright front that propagated continuously from an active region across the solar surface and that was associated with a CME. The source active region was the only active region present on the solar surface. The ejection occurred near solar minimum, when the Sun's magnetic field was mainly dipolar. A dimming area developed between the bright front and the active region. A brightening developed at the edge of the coronal hole and remained at the same location for at least 6 hr. On 1998 June 13 a moving arch and a stationary bright front were both observed. The moving arch appears similar to the EIT wave described by Thompson et al. (1998) since they are both moving arches and since they both involve the appearance of similar structures and the eruption of a filament. The motion of the magnetic flux tube where the filaments are lying may push the surrounding magnetic field, producing plasma compression and electric currents that can locally produce brightenings. The main difference between the two events resides in the large-scale magnetic field topology; on 1997 May 12 the solar magnetic field is mainly dipolar, and on 1998 June 13 it is mainly quadrupolar.

Stationary bright fronts that are shown in this paper seem to be related to the large-scale magnetic field topology. The footpoints of the magnetic separatrixes in the typical quadrupolar magnetic configuration of a rather active Sun (Wang et al. 1997; Banaszkiewicz, Axford, & McKenzie 1998; Delannée & Aulanier 1999) can lie where the stationary bright fronts are, near the equator. Delannée & Aulanier (1999) showed the importance of the magnetic field line connectivity and of the separatrixes due to a multipolar topology for a plausible explanation of the overall structures observed on 1997 November 3. Further support for the importance of the magnetic field topology is provided by the magnetic break-out model (Antiochos et al. 1999). This model predicts how quadrupolar magnetic fields can evolve into open magnetic field lines via reconnection of magnetic field lines of different connectivities in the separatrix layer. During the motion of the magnetic field lines electric currents are formed in the separatrixes that may produced heating and therefore brightening of the plasma in 195 Å. Moreover, the brightenings observed on 1997 May 12 (Thompson et al. 1998) are located at the interface between the open and closed magnetic field, i.e., in a separatrix, indicating again the importance of the separatrixes in the EIT waves.

## 5. CONCLUSION

Thompson et al. (1998) and Delannée & Aulanier (1999) found that brightenings produced by CMEs were located at the footpoints of separatrixes. The brightenings of transequatorial loops and the stationary bright front described in this paper may have been due to the interaction of magnetic field lines with different connectivities before the eruption. The moving arch could originate from the interaction between sheared expanding magnetic field lines with surrounding magnetic field lines that are nearly potential (Delannée & Amari 2000). This magnetic field line interaction could produce local electric currents and pressure increases that could be observed as brightenings. The stationary bright fronts, the 1997 May 12 brightenings, and the arches seem to be due to two different parts of the magnetic structure involved in a CME.

We would like to thank B. J. Thompson, G. Aulanier, and T. Amari for helpful discussions. This work was performed while the author held a National Research Council NASA/Goddard Space Flight Center Research Associateship.

REFERENCES

Amari, T., Luciani, J.-F., Aly, J.-J., & Tagger, M. 1996, A&A, 306, 913
Antiochos, S. K., DeVore, C. R., & Klimchuk, J. A. 1999, ApJ, 510, 485
Aulanier, G., Démoulin, P., Schmieder, B., Fang, C., & Tang, Y. H. 1998, Sol. Phys., 183, 369
Banaszkiewicz, M., Axford, W. I., & McKenzie, J. F. 1998, A&A, 337, 940
Brueckner, G. E., et al. 1995, Sol. Phys., 162, 357
Bungey, T. N., Titov, V. S., & Priest, E. R. 1996, A&A, 308, 233
Delaboudinière, J.-P. et al. 1995, Sol. Phys., 162, 291
Delannée, C., & Amari, T. 2000, ApJL, submitted
Delannée, C., & Aulanier, G. 1999, Sol. Phys., 190, 107
Delannée, C., Delaboudinière, J.-P., & Lamy, P. 2000, A&A, 355, 725
Démoulin, P., Bagalá, L. G., Mandrini, C. H., Hénoux, J.-C., & Rovira, M. G. 1997, A&A, 325, 305
Handy, B. N., et al. 1999, Sol. Phys., 187, 229
Hudson, H. S., Acton, L. W., & Freeland, S. L. 1996, ApJ, 470, 629
Karpen, J. T., Antiochos, S. K., DeVore, C. R., & Golub, L. 1998, ApJ, 495, 491
Khan, J. I., & Hudson, H. S. 2000, Geophys. Res. Lett., 27, 1083
Khan, J. I., Uchida, Y., McAllister, A. H., Mouradian, Z., Soru-Escaut, I., & Hiei, E. 1998, A&A, 336, 753
Maia, D., Voulidas, A., Pick, M., Howard, R., Schwenn, R., & Magalhães, A. 1999, J. Geophys. Res., 104A6, 12.507
Manoharan, P. K., van Driel-Gesztelyi, L., Pick, M., & Demoulin, P. 1996, ApJ, 468, L73
Martres, M.-J. 1989, Sol. Phys., 119, 357
Milano, L. J., Dmitruk, P., Mandrini, C. H., Gómez, D. O., & Démoulin, P. 1999, ApJ, 521, 889
Solodyna, C. V., Krieger, A. S., & Nolte, J. T. 1977, Sol. Phys., 54, 123
Thompson, B. J., et al. 1999, ApJ, 517, L151
Thompson, B. J., Plunkett, S. P., Gurman, J. B., Newmark, J. S., St. Cyr, O. C., & Michels, D. J. 1998, Geophys. Res. Lett., 25, 2465
Thompson, B. J., Reynolds, B., Aurass, H., Gopalswamy, N., Gurman, J. B., Hudson, H. S., Martin, S. F., & St. Cyr, O. C. 2000, Sol. Phys., 193, 161
Titov, V. S., & Démoulin, P. 1999, A&A, 351, 707
Uchida, Y. 1968, Sol. Phys., 4, 30
Wang, Y.-M., et al. 1997, ApJ, 479, 448
Wills-Davey, M., & Thompson, B. J. 1999, Sol. Phys., 190, 467
Zarro, D. M., Sterling, A. C., Thompson, B. J., Hudson, H. S., & Nitta, N. 1999, ApJ, 520, L139